Am J Clin Exp Immunol 2025;14(2):68-85
www.ajcei.us /ISSN:2164-7712/AJCEI0162236

Original Article

Bioinformatics analysis of FCER1A as a key immune marker in dilated cardiomyopathy and systemic lupus erythematosus

Li Xu*, Tao Wu*, Wu Zhang, Songlin Xiao

Department of Cardiovascular Medicine, People's Hospital of Anyue County, Ziyang 642350, Sichuan, PR China.
**Equal contributors.*

Received November 24, 2024; Accepted April 6, 2025; April 25, 2025; Published April 30, 2025

Abstract: Background: Systemic lupus erythematosus (SLE) and dilated cardiomyopathy (DCM) are closely linked biologically, especially regarding immune responses. However, key biomarkers mediating the onset and development of both diseases are still lacking. This study uses bioinformatic methods to analyse the immune microenvironment of the ventricles of DCM patients and to search for biomarkers related to DCM and SLE. Methods: Single-cell and bulk transcriptomic data for DCM were obtained from the GEO database, while GWAS data for SLE were obtained from the FinnGen database. The SMR method was used to identify genetic variants in the ventricles associated with SLE. Differential analysis was used to detect genes specific to monocyte-macrophages. Subsequently, a combination of machine learning algorithms was employed to select hub genes. Finally, small molecule drugs targeting the hub genes were retrieved from the DGIdb database. Results: Mononuclear macrophages were found to be significantly infiltrated in dilated cardiomyopathy (DCM) samples. Seven key genes (HLA-DQB1, CD52, FCER1A, etc.) were identified by cross-tabulation analysis, of which FCER1A was the best-performing (AUC 0.8-0.9) among ten machine learning models. Validation of multiple datasets showed that FCER1A was highly expressed in the DCM group, was mainly involved in the immune cell activation pathway, and strongly interacted with other cells in the myocardial microenvironment through the MK/PROS pathway. The gene was highly expressed in the middle and late stages of monocyte-macrophage differentiation and was associated with drugs such as benzathine penicillin polylysine and omalizumab. Conclusion: FCER1A was found to be a key differentially expressed gene in mononuclear macrophages in DCM myocardial tissue, and its significantly high expression was closely associated with immune cell activation in the myocardial microenvironment, which lays a theoretical foundation for immunotherapy of DCM and requires further clinical validation.

Keywords: Dilated cardiomyopathy, immune infiltration, diagnosis, bioinformatics, mononuclear macrophage, single-cell sequencing analyze

Introduction

Dilated cardiomyopathy (DCM) is a common heart muscle disease characterised by the dilation and impaired contraction of the left ventricle, leading to heart failure [1]. The epidemiology of DCM suggests a prevalence of 1 in 2500 individuals, with a complex interplay of genetic and environmental factors contributing to its development [2]. The aetiology of DCM is multifaceted, encompassing viral infections, autoimmune diseases, and genetic mutations [3]. Clinically, DCM presents with symptoms of dyspnoea, fatigue and peripheral oedema, which can progress to severe heart failure if left untreated [4]. Current treatment strategies for DCM include pharmacological interventions, device-based therapies and surgical options to improve cardiac function and patient survival [5].

Systemic lupus erythematosus (SLE) is an autoimmune disease that affects multiple organ systems, including the skin, joints, kidneys, and cardiovascular system [6]. The association between SLE and DCM is of significant clinical interest, as patients with SLE are at an increased risk of developing DCM due to shared

https://doi.org/10.62347/KGZR5419

pathogenic mechanisms such as chronic inflammation and immune dysregulation [7].

The association between SLE and DCM is well documented in the literature. SLE is a systemic autoimmune disease characterised by the production of autoantibodies that target various organs and tissues, including the heart. The presence of autoantibodies in SLE can lead to the development of myocarditis, which can progress to DCM [8]. In addition to myocarditis, SLE can also cause other cardiovascular complications, such as pericarditis, valvular heart disease, and coronary artery disease, which can contribute to the development of DCM [9]. The pathogenesis of DCM in the context of SLE is thought to involve a combination of immune-mediated myocardial damage, inflammation, and fibrosis.

The role of bioinformatics in the study of DCM and SLE has been increasingly recognised in recent years. In the context of SLE, bioinformatics has been used to study the genetic basis of the disease, identify susceptibility loci, and understand the molecular mechanisms involved in the pathogenesis of SLE-related cardiovascular complications. In the context of DCM, bioinformatics tools have been used to analyse gene expression data, identify differentially expressed genes, and discover novel biomarkers. Therefore, this paper aims to screen and obtain biomarkers that play important functions in SLE and DCM using bioinformatics methods.

Materials and methods

Data collection

The single-cell sequencing dataset (GSE135337) was obtained from the Gene Expression Omnibus (GEO) database, which included 5 DCM samples and 2 NF samples [10]. A total of 49723 ventricular cells were included in our analysis. After annotation, a total of 183 B cells, 11576 endothelial cells, 23549 fibroblasts, 37 lymphocytes, 4371 mononuclear/macrophages, 315 neurons cells, 414 NK cells, 5683 pericytes, 888 smooth muscle cells and 2347 T cells were obtained. The bulk RNA sequencing data (GSE141910, GSE57345, GSE116250 and GSE42955) for this study were obtained from the Gene Expression Omnibus (GEO) database. A total of 297 NF samples and 321 DCM samples were included and analysed [11-17].

SMR data

Expression Quantitative Trait Loci (eQTL) are genetic variants or single nucleotide polymorphisms (SNPs) that influence gene expression levels. These genetic loci are associated with the expression levels of specific genes in individual genomes. Studying eQTL provides insights into the genetic factors regulating gene expression, revealing gene functionality and its association with phenotypes. A key resource is the Genotype-Tissue Expression (GTEx) project, which collects tissue samples from a variety of healthy individuals, including organs such as heart, liver, kidney, lung and brain. With contributions from thousands of donors, GTEx offers extensive eQTL data, elucidating the relationship between genotypes and gene expression levels. Our analysis focuses on the GTEx V8 Heart_Left_Ventricle eQTL summary statistics and finngen_R7_M13_SLE for SMR analysis, which includes 538 case samples and 213145 control samples [18].

SMR analysis

In this analysis, we used summary data-based Mendelian randomisation (SMR) to investigate whether single nucleotide polymorphisms (SNPs) influencing phenotype are mediated by gene expression. We used summary data from genome-wide association studies (GWAS) and expression quantitative trait loci (eQTL) studies to explore the association between gene expression and SLE. In addition, we performed a Heterogeneity in Dependent Instruments (HEIDI) test to assess whether the observed associations were influenced by linkage disequilibrium. A P_HEIDI value less than 0.05 indicates that the observed associations may be due to two independent genetic variants in linkage disequilibrium. Genes with P_SMR less than 0.05 and P_HEIDI greater than 0.05 are considered statistically significant. The analysis was performed using version 1.3.1 of the SMR software tool [19].

Functional enrichment analysis

The Gene Ontology (GO) and Kyoto Encyclopedia of Genes and Genomes (KEGG) systems provide structured, computable information on

the functionality of genes and gene products. Functional enrichment analysis was conducted using the R package clusterProfiler [20], and enrichment analysis results were visualised. A significance threshold of P<0.05 was used.

Differential gene expression analysis

Differential gene expression analysis was performed on the gene expression data of DCM patients from GSE141910 using the limma package in R [21]. Genes meeting the criteria of adj_*P*.value <0.05 and |LogFC| >1 were categorised as differentially expressed. A volcano plot was generated from this analysis using the "ggplot" package.

Assessing the tumor immune microenvironment

To comprehensively assess the extent of immune infiltration, we used a variety of bioinformatics algorithms, including single-sample gene set enrichment analysis (ssGSEA), tumour immune estimation resource (TIMER), cell type identification by estimating relative subsets of RNA transcripts (CIBERSORT), QUANTISEQ, Estimate, microenvironment cell population counter (MCPcounter), Xcell, and immune and cancer cell proportion estimation (EPIC). Note that these algorithms are encapsulated in the R package IOBR, which is called directly for immune infiltration analysis in this study [22]. Each algorithm uses unique strategies and gene expression characteristics to estimate the abundance of different immune cell subsets. By calculating the enrichment or relative abundance of marker genes, we accurately estimated the proportion of immune cell types in the ventricular samples. In addition, a heat map was drawn using the ComplexHeatmap R package [23].

Cell communication analysis

To explore crosstalk patterns between cells, we used the R package CellChat. We first created CellChat objects from the normalised count matrix using a standardised workflow. Next, we used the identify overexpressed genes and identify overexpressed interactions functions to process the data with default settings. We then used the compute CommunProb, compute CommunProb Pathway and aggregateNet functions to evaluate and analyse potential ligand-receptor (L/R) interactions between all cells, with a particular focus on interactions between cell types in DCM and NF ventricular [24].

Establishment of tow-classification mechanical learning models

When classifying the binary categories of DCM, we employed feature selection methods to identify key features. Following a 7:3 ratio, 232 samples from the GSE141910 dataset were divided into training and validation groups. To ensure consistency and efficiency in the modelling process, we consistently used the caret package in R for model building [25]. This package provides a variety of modelling functions, including glmnet, GBM, avNNet, logitboost, NB, PAM, ctree, RF, and KNN. Minimising errors in the model prediction process depends on determining the optimal hyperparameters for each algorithm. Fortunately, the caret package simplifies this process by defaulting to a standard grid set for automatically tuning the hyperparameters of each algorithm. Once these parameters are identified, they are applied to the down-sampled training data set to fit the model parameters. We then evaluate the performance of the model on the test dataset. To ensure the accuracy of the model training, we use 10 cross-validation to select the best parameter set, providing a solid foundation for the final predictions.

Statistical analysis

Statistical analyses were performed for the significance of differences and correlations observed in the study. All data are expressed as mean ± standard deviation (SD). Pearson correlation analysis was performed to explore relationships between variables. Statistical analysis and scientific plotting were performed using R Studio (version 4.3.3). A significance level of P<0.05 was considered statistically significant.

Results

The crucial role of mononuclear macrophages in the development of DCM

All data sources for the article are shown in **Table 1**. After preliminary processing, the UMAP results of the cells in each sample are shown in **Figure 1A**, indicating no obvious batch

Table 1. Data sources

Dataset	Category	N sample	Data_type	Population
GSE183852	Transmittal LV Apex	NF:2 DCM:5	scRNA-seq	European
GSE141910	Left ventricle	NF:166 DCM:166	RNA-seq	European
GSE57345	Left ventricle	NF:136 DCM:82	Microarray	European
GSE116250	Left ventricle	NF:14 DCM:37	RNA-seq	European
GSE42955	Left ventricle	NF:5 DCM:12	Microarray	European
Finngen_R7_M13_SLE	Binary	Case:538 Comtrol:213145		Europea

effects within the samples. **Figure 1B** shows that after dimension reduction and clustering, all cells can be distinctly divided into 26 clusters with clear differences between them. The annotated cell UMAP results are shown in **Figure 1C**, with the marker genes expressed by relevant cells as depicted in **Figure 1D**. Monocytes and macrophages are grouped together for ease of further investigation. The enrichment analysis of marker genes for each cell type is shown in **Figure 1E**, indicating that the marker genes of each cell subset can be clearly distinguished, and the pathways enriched by cell subsets are essentially similar to those recognised by cell subsets such as B cells: B cell differentiation; mononuclear macrophages: immune response, bacterial defence and complement activation. The proportions of cell types in the ventricular cells are shown in **Figure 1F**, **1G** and show that in the ventricle, fibroblasts are significantly decreased in DCM, whereas mononuclear macrophages are significantly increased, suggesting that mononuclear macrophages may play an important role in the development of DCM. For key pathways involved in the development of DCM, such as NOTCH, INTRINSIC_APOPTOTIC and TGFB, the Addmodelscore algorithm is used for scoring, and their enrichment in various cell populations is shown in **Figure 1H**, indicating that mononuclear macrophages show high expression in all three pathways, suggesting their important role in the development of DCM.

Identification of key genes

For the differential analysis of DCM and NF samples from the GSE183852 dataset, the results are shown in **Figure 2A**. Based on the criteria of avg_log2FC >1 and p_val_adj <0.05, 2653 differentially expressed genes were identified in the DCM group; to identify the characteristic genes of mononuclear macrophages, we performed differential analysis based on different cell types. The results are shown in **Figure 2B**. Based on the criteria of avg_log2FC >1 and p_val_adj <0.05, 1874 characteristic genes highly expressed in mononuclear macrophages were identified; to identify SLE-related genes, we conducted an MR analysis based on summary data (SMR analysis) for SLE. By summarising the results of genome-wide association studies (GWAS), we applied a specific MR analysis technique, summary data SMR analysis. After SVR analysis, the Manhattan plot of SLE-related genes is obtained (**Figure 2C**), and 210 SLE-related genes were selected based on the criteria of p_SMR <0.05 and p_HEID >0.05. By taking the intersection of differentially expressed genes in the DCM group, characteristic genes of mononuclear macrophages, and SLE-related genes, a total of 7 key intersected genes were obtained for subsequent analysis, namely HLA-DQB1, CD52, FCER1A, HLA-DQB2, WDFY4, CSGALNACT2, and NCR3LG1 (**Figure 2D**).

Hub gene selection using multiple machine learning algorithms

To identify the hub genes that play a significant role in DCM from the above seven intersected genes, we used several machine learning algorithms. We used DCM and NF as target variables and the expression of the intersected genes as independent variables to build and

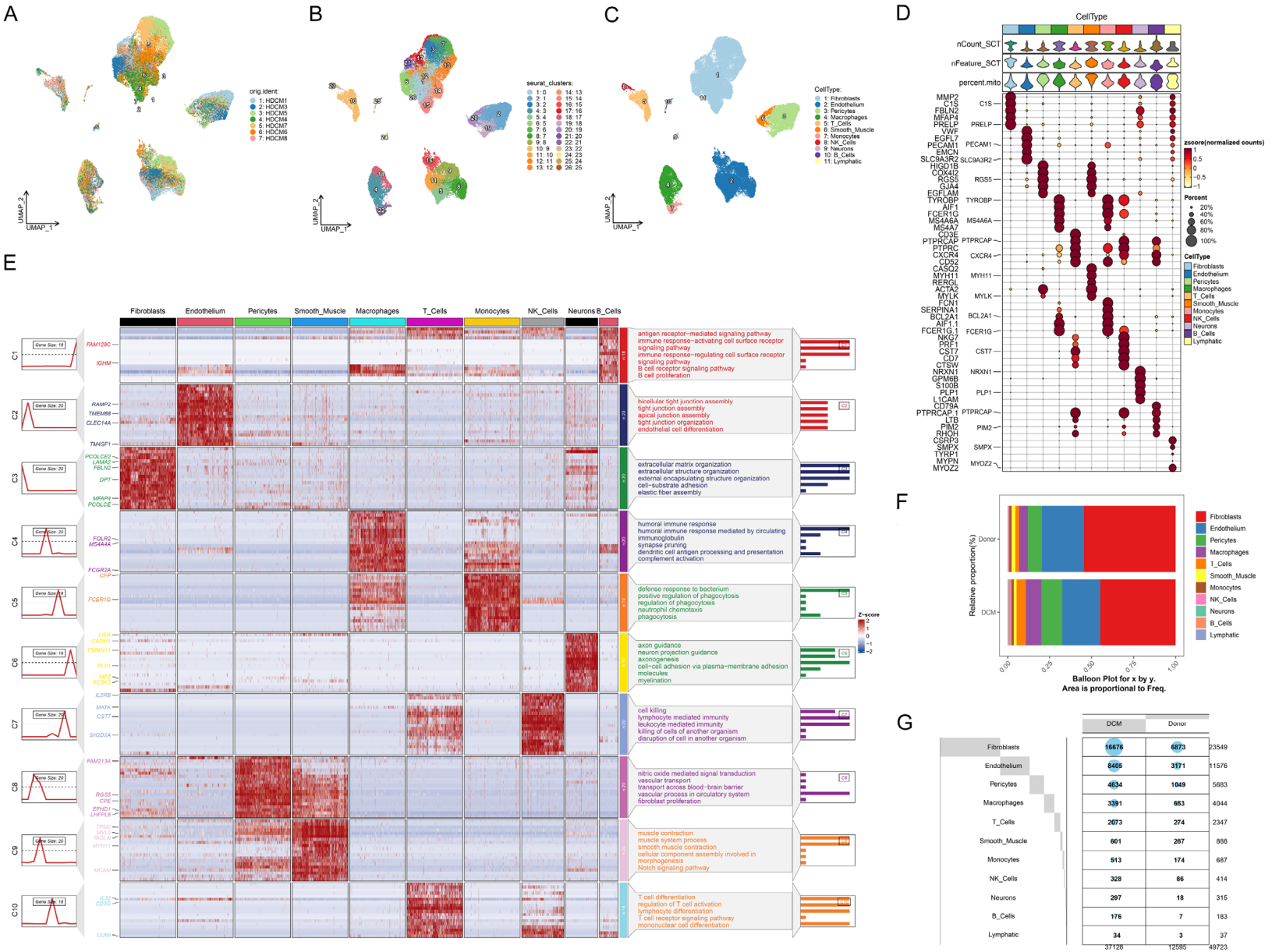
A
B
C
D
E
F
G
UMAP_1
UMAP_2
orig.ident:
1: HDCM1
2: HDCM3
3: HDCM5
4: HDCM4
5: HDCM7
6: HDCM6
7: HDCM8
seurat_clusters:
CellType:
1: Fibroblasts
2: Endothelium
3: Pericytes
4: Macrophages
5: T_Cells
6: Smooth_Muscle
7: Monocytes
8: NK_Cells
9: Neurons
10: B_Cells
11: Lymphatic
CellType
nCount_SCT
nFeature_SCT
percent.mito
zscore(normalized counts)
Percent
Fibroblasts
Endothelium
Pericytes
Macrophages
T_Cells
Smooth_Muscle
Monocytes
NK_Cells
Neurons
B_Cells
Lymphatic
Relative proportion(%)
Donor
DCM
Balloon Plot for x by y.
Area is proportional to Freq.
Z-score
antigen receptor−mediated signaling pathway
immune response−activating cell surface receptor signaling pathway
immune response−regulating cell surface receptor signaling pathway
B cell receptor signaling pathway
B cell proliferation
bicellular tight junction assembly
tight junction assembly
apical junction assembly
tight junction organization
endothelial cell differentiation
extracellular matrix organization
extracellular structure organization
external encapsulating structure organization
cell−substrate adhesion
elastic fiber assembly
humoral immune response
humoral immune response mediated by circulating immunoglobulin
synapse pruning
dendritic cell antigen processing and presentation
complement activation
defense response to bacterium
positive regulation of phagocytosis
regulation of phagocytosis
neutrophil chemotaxis
phagocytosis
axon guidance
neuron projection guidance
axonogenesis
cell−cell adhesion via plasma−membrane adhesion molecules
myelination
cell killing
lymphocyte mediated immunity
leukocyte mediated immunity
killing of cells of another organism
disruption of cell in another organism
nitric oxide mediated signal transduction
vascular transport
transport across blood−brain barrier
vascular process in circulatory system
fibroblast proliferation
muscle contraction
muscle system process
smooth muscle contraction
cellular component assembly involved in morphogenesis
Notch signaling pathway
T cell differentiation
regulation of T cell activation
lymphocyte differentiation
T cell receptor signaling pathway
mononuclear cell differentiation
DCM
Donor
Fibroblasts 16676 6873 23549
Endothelium 8405 3171 11576
Pericytes 4634 1049 5683
Macrophages 3391 653 4044
T_Cells 2073 274 2347
Smooth_Muscle 601 287 888
Monocytes 513 174 687
NK_Cells 328 86 414
Neurons 297 18 315
B_Cells 176 7 183
Lymphatic 34 3 37
37128 12595 49723

H

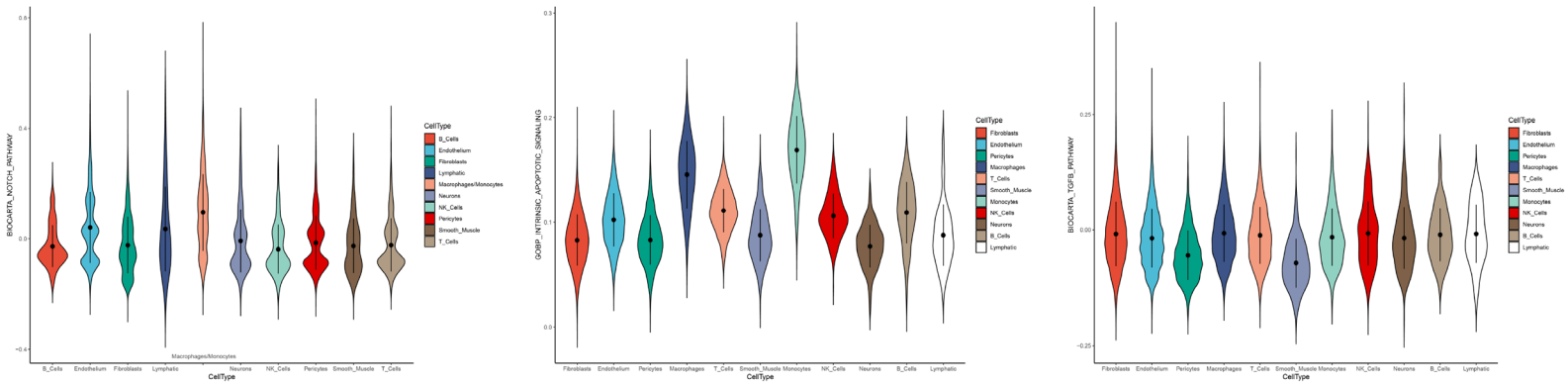

Figure 1. Deciphering the microenvironment of DCM ventricular cells. A. UMAP plot of cells grouped by sample condition. B. UMAP plot of cells grouped by cluster condition. C. UMAP plot of cell clusters. D. Bubble plot of cell cluster marker gene annotations. E. Heatmap of cell cluster marker genes and enrichment. F. Stacked bar plot of cell subset proportions grouped by NF and DCM. G. Distribution of cell subset proportions. H. Enrichment of DCM-related pathways in cell clusters.

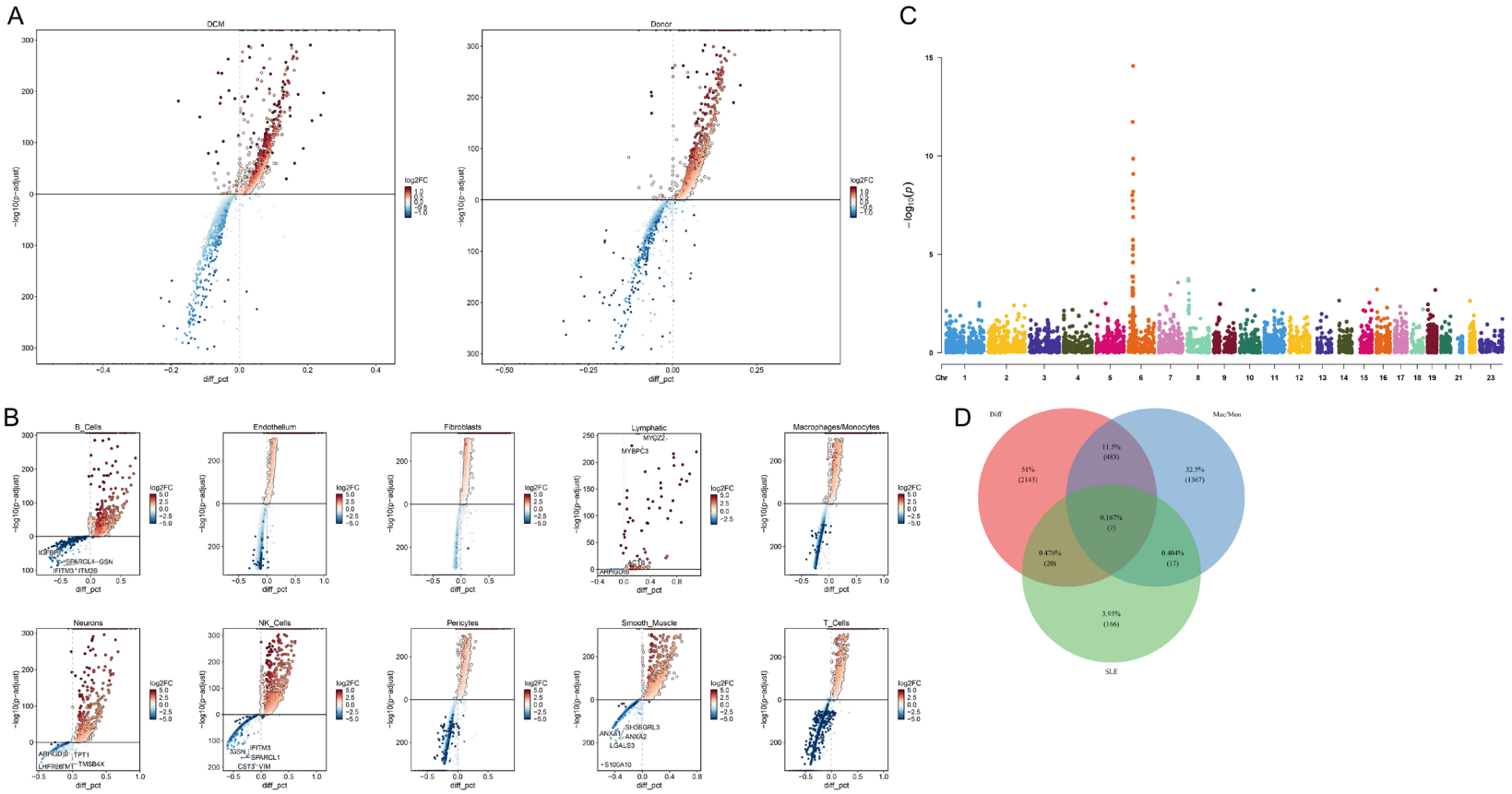

Figure 2. Identification of key genes in DCM macrophages and SLE. A. Identification of differential genes grouped by DCM and NF. B. Identification of key genes in macrophages grouped by cell subset. C. SMR analysis of SLE genetic variant sites. D. Intersection of differential genes, key macrophage genes, and key SLE genetic variant sites.

evaluate models to estimate the importance of the variables. Initially, we observed the expression patterns of intersected genes between DCM and NF groups. As shown in **Figure 3A**, FCER1A, CD52, HLA-DQB1, HLA-DQB2, and WDFY4 were highly expressed in the DCM group, while CSGALNACT2 and NCR3LG1 were highly expressed in the NF group. The efficacy metrics of the ten models are shown in **Figure 3B**, indicating that the glmnet model had the highest ROC, sensitivity, and specificity, with an ROC metric greater than 0.9 in the training set, suggesting its excellent performance (**Figure 3C**). Subsequently, we examined the variable importance ranking in five models, as shown in **Figure 3D**. Notably, the FCER1A gene showed the best performance in all models, indicating the highest variable importance level. The calibration curve in the validation set, shown in **Figure 3E**, suggests an increasing trend in the observed number of events as the bin midpoint increases. Moreover, for the PAM and glmnet models, the AUC in both the validation and training sets was greater than 0.85, indicating the good diagnostic efficacy of the trained models (**Figure 3F**).

Feature analysis of FCER1A

We observed the differential expression of FCER1A in several DCM and NF datasets. As shown in **Figure 4A**, the gene was significantly highly expressed in DCM samples in the GSE141910, GSE116250, and GSE57345 datasets ($P<0.05$). In addition, FCER1A also showed a trend towards higher expression in the DCM group in the GSE42955 dataset. The single cell expression UMAP results for FCER1A are shown in **Figure 4B**, indicating its primary expression in mononuclear macrophages, with a significant difference in expression in other cell types, further validating it as a characteristic gene of mononuclear macrophages ($P<0.05$). Moreover, FCER1A also showed higher expression in the DCM group compared to the NF group in single-cell data, confirming the expression characteristics of FCER1A obtained from conventional transcriptomics (**Figure 4C**, **4D**). Subsequently, regarding the effector site situation of FCER1A in SLE, we found that FCER1A is positively correlated with the risk of developing SLE and can serve as a risk factor for the disease (**Figure 4E**). The site localisation situation further confirms that FCER1A can act as an independent negative factor promoting the development of SLE (**Figure 4F**).

Functional analysis of FCER1A differences

To explore the pathways through which FCER1A functions in DCM, we selected the DCM samples in the GSE141910 dataset and stratified them based on the top and bottom 30% expression of this gene. The PCA results after stratification are shown in **Figure 5A** and show a clear heterogeneity between the two groups. Using FCER1A as the control group and setting $|log2FC| >1$ and $adj\_pvalue <0.05$ as the threshold, a total of 265 upregulated differential genes and 84 downregulated differential genes were identified as shown in **Figure 5B**. The heat map shows that the obtained differential genes can be significantly clustered into two categories (Cluster1 and Cluster2) under unsupervised clustering conditions, and overall, the expression trends of genes in each cluster are markedly opposite (**Figure 5C**). The GO and KEGG enrichment analysis results for upregulated genes are shown in **Figure 5D**, **5E**, indicating that FCER1A primarily functions by upregulating immune-related pathways such as chemokine receptor activity, lymphocyte differentiation, and PI3K. The GO and KEGG enrichment analysis results for downregulated genes are shown in **Figure 5F**, **5G**, indicating that in DCM patients with low expression of FCER1A, one-carbon unit, oxygen, and lipid transport can be upregulated. And the GSEA results are shown in **Figure 5H-K**. Overall, upregulated differential genes are mainly enriched in immune activation-related pathways, such as the differentiation and development of T and B cells, chemokine communication, Th17 activation, and immune regulatory interactions. Downregulated differential genes are mainly enriched in substance metabolism and transport-related pathways, such as ATP synthesis coupled to electron transport, peptide chain elongation and respiratory chain electron transport.

Immune microenvironment decoding

Firstly, we observed the differences in immune cell composition between the ventricles of DCM patients and NF normal samples. The results, as shown in **Figure 6A**, indicate that most immune cells in the ventricles of DCM patients are highly infiltrated. Compared to the FCER1A_

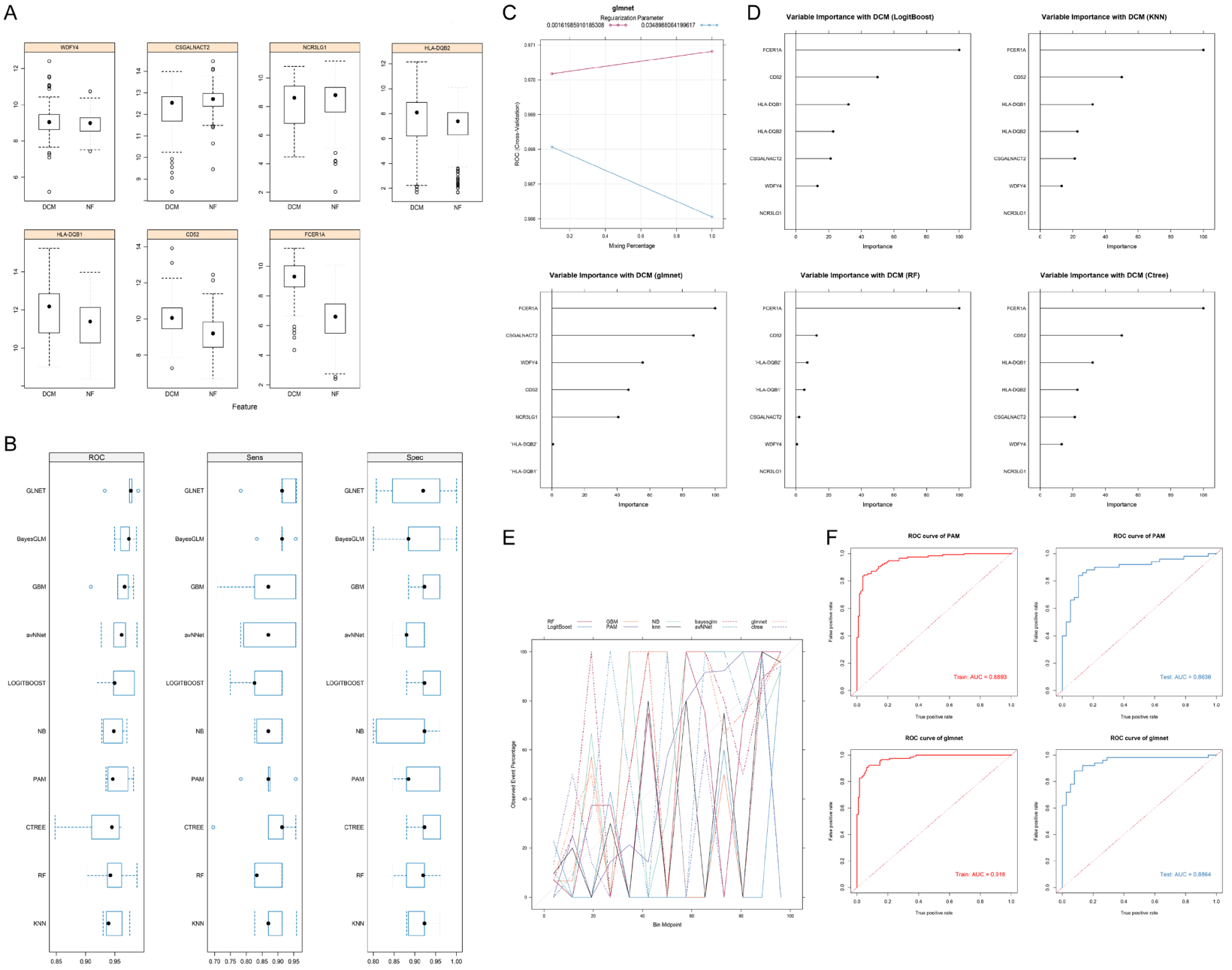
A
WDFY4
CSGALNACT2
NCR3LG1
HLA-DQB2
HLA-DQB1
CD52
FCER1A
DCM
NF
Feature
B
ROC
Sens
Spec
GLNET
BayesGLM
GBM
avNNet
LOGITBOOST
NB
PAM
CTREE
RF
KNN
C
glmnet
Regularization Parameter
0.00161585910185308
0.0348986064199617
ROC (Cross-Validation)
Mixing Percentage
D
Variable Importance with DCM (LogitBoost)
Variable Importance with DCM (KNN)
Variable Importance with DCM (glmnet)
Variable Importance with DCM (RF)
Variable Importance with DCM (Ctree)
Importance
E
RF
LogitBoost
GBM
PAM
NB
knn
bayesglm
avNNet
glmnet
ctree
Observed Event Percentage
Bin Midpoint
F
ROC curve of PAM
Train: AUC = 0.8893
Test: AUC = 0.8636
ROC curve of glmnet
Train: AUC = 0.918
Test: AUC = 0.8864
False positive rate
True positive rate

Figure 3. Hub gene selection by multiple machine learning methods. A. Expression of intersection genes in DCM and NF groups. B. Sensitivity, specificity, and ROC curve analysis of multiple machine learning algorithms. C. GLMnet model situation. D. Variable importance in models under five machine learning algorithms. E. Calibration curve of the model within the test set. F. ROC curves of the PAM and GLMnet algorithms within the test and validation sets.

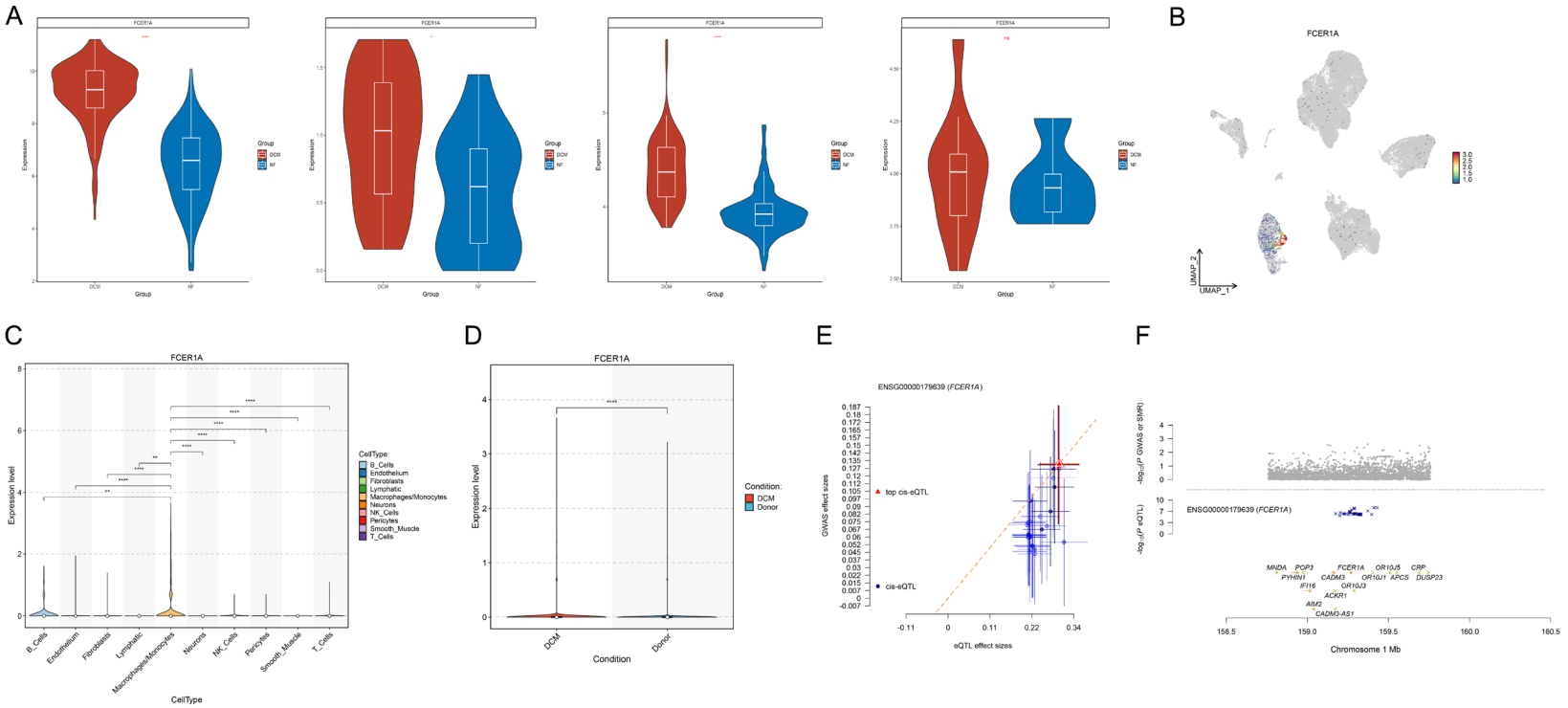

Figure 4. Characteristic analysis of the FCER1A gene. A. Violin plots showing the expression difference of FCER1A in GSE141910, GSE116250, GSE57345, and GSE42955 from left to right. B UMAP plot of FCER1A expression distribution. C. Violin plots of FCER1A expression difference in different cell subsets. D. Differential expression of FCER1A in different sample groups. E. Effector location of FCER1A in SLE. F. Effector site of FCER1A.

FCER1A as a key immune marker in SLE and DCM

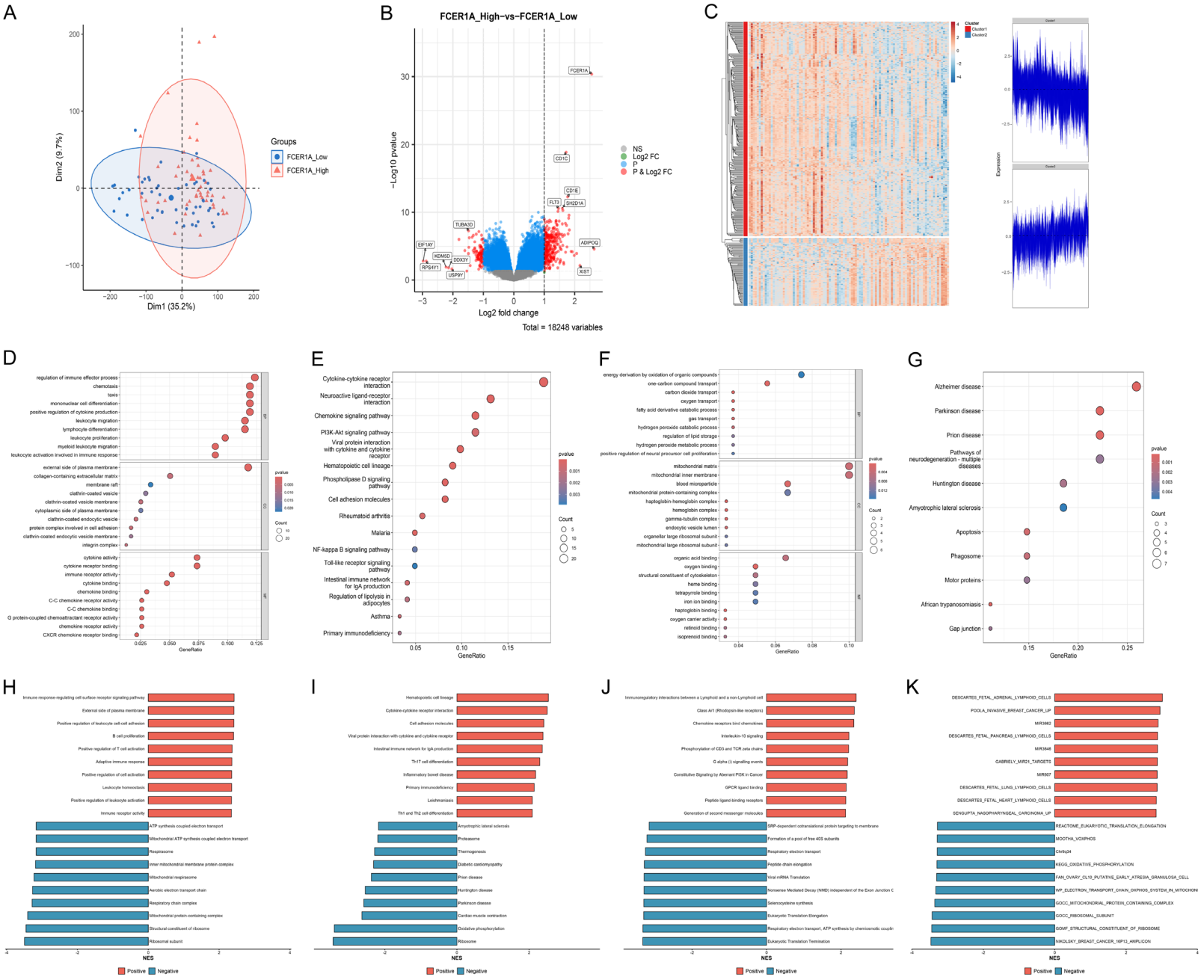

Figure 5. Functional analysis of FCER1A in DCM. A. PCA dimension reduction of samples grouped by the top and bottom 30% of FCER1A expression in DCM. B. Volcano plot of differential analysis between FCER1A_High and FCER1A_Low groups. C. Expression heatmap of differential genes selected by abs(logFC) >1 and adj.pvalue <0.05. D. GO enrichment of up-regulated differential genes. E. KEGG enrichment of up-regulated differential genes. F. GO enrichment bubble chart of down-regulated differential genes. G. KEGG enrichment bubble chart of downregulated differential genes. H-K. GSEA enrichment bar chart of differential genes in GO (H), KEGG (I), Reactome (J) and Msidb (K) databases.

Low group, the FCER1A_High group has significantly higher infiltration levels of NK cells, CD4+ T cells, CD8+ T cells, B cells, and monocytes. Regarding macrophage infiltration, we found that the FCER1A_High group has a higher infiltration level, such as Macrophage_xCell and Macrophage_quantiseq (**Figure 6B**). In addition, we observed that various immune-related features are highly expressed in the DCM group compared to the NF group ventricular cells, with features such as TNF, TIP, ICB, MHC molecules, HLA and others showing higher expression (**Figure 6C**). For the FCER1A_High group, we found that this group down-regulates the expression of several immune-related features, such as TIP, MDSC, BCR, and TCR (**Figure 6D**).

FCER1A+ macrophage microenvironment analysis

To observe the function of FCER1A- mediated mononuclear macrophages in the ventricular microenvironment, we divided them into FCER1A+ macrophages and FCER1A- macrophages. The overall interaction strength is shown in **Figure 7A**, **7B**, suggesting that FCER1A+ macrophages have stronger interaction intensity compared to FCER1A- macrophages, such as NK cells, fibroblasts and lymphocytes. **Figure 7C** shows the difference in the receptor-ligand level enriched by various cell types, indicating that FCER1A- Macrophage has the strongest ability as a signal receiver. In terms of signal emission capability, and FCER1A+ Macrophage has a stronger enrichment level in the PROS, MK, CXCL, and GAS signal pathways compared to FCER1A- Macrophage (**Figure 7D**). For the two significantly different pathways, namely MK and PROS, the analysis results are shown in **Figure 7E**, **7F**, indicating that in the MK pathway, FCER1A+ Macrophage has a strong interaction with NK cells and other cell groups, while in the PROS pathway, FCER1A- Macrophage has no interaction with other cell types, while FCER1A+ Macrophage has an interaction with NK cells and peripheral cells. To observe the relationship between the expression of FCER1A and macrophage differentiation, we performed pseudotime analysis on macrophages. The results are shown in **Figure 7G**, which indicates that FCER1A is mainly significantly expressed in the middle and late stages of macrophage differentiation. **Figure 7H** shows that FCER1A, which is co-expressed in the middle and late stages of macrophage differentiation, is mainly enriched in the regulation of protein activity and type II interferon production.

FCER1A small molecule drug screening

To identify small-molecule drugs targeting FCER1A. We used the DGIdb database to search for drugs targeting the FCER1A gene, the results are shown in **Figure 8A**, indicating that a total of two approved drugs were obtained, namely BENZYLPENICILLOYL POLYLYSINE and OMALIZUMAB. The former is mainly used for treating allergic reactions and as a diagnostic agent, while the latter is a recombinant humanized monoclonal antibody targeting anti-IgE, mainly used for treating moderate to severe asthma. In addition, we also use a network diagram to show the interaction relationship between the target FCER1A and small molecule drugs (**Figure 8B**).

Discussion

Heart failure is a complex clinical syndrome caused by the dysfunction of various biological processes leading to cardiac dysfunction [26]. In this study, we started from a single cell perspective and found that mononuclear macrophages in the DCM group showed significantly increased infiltration compared to NF samples. Based on this finding, we identified specific expression genes in mononuclear macrophages and differential genes in the DCM group compared to the NF group. Additionally, using SMR analysis, we obtained significant genetic variants that are highly associated with the occurrence of SLE. The seven overlapping

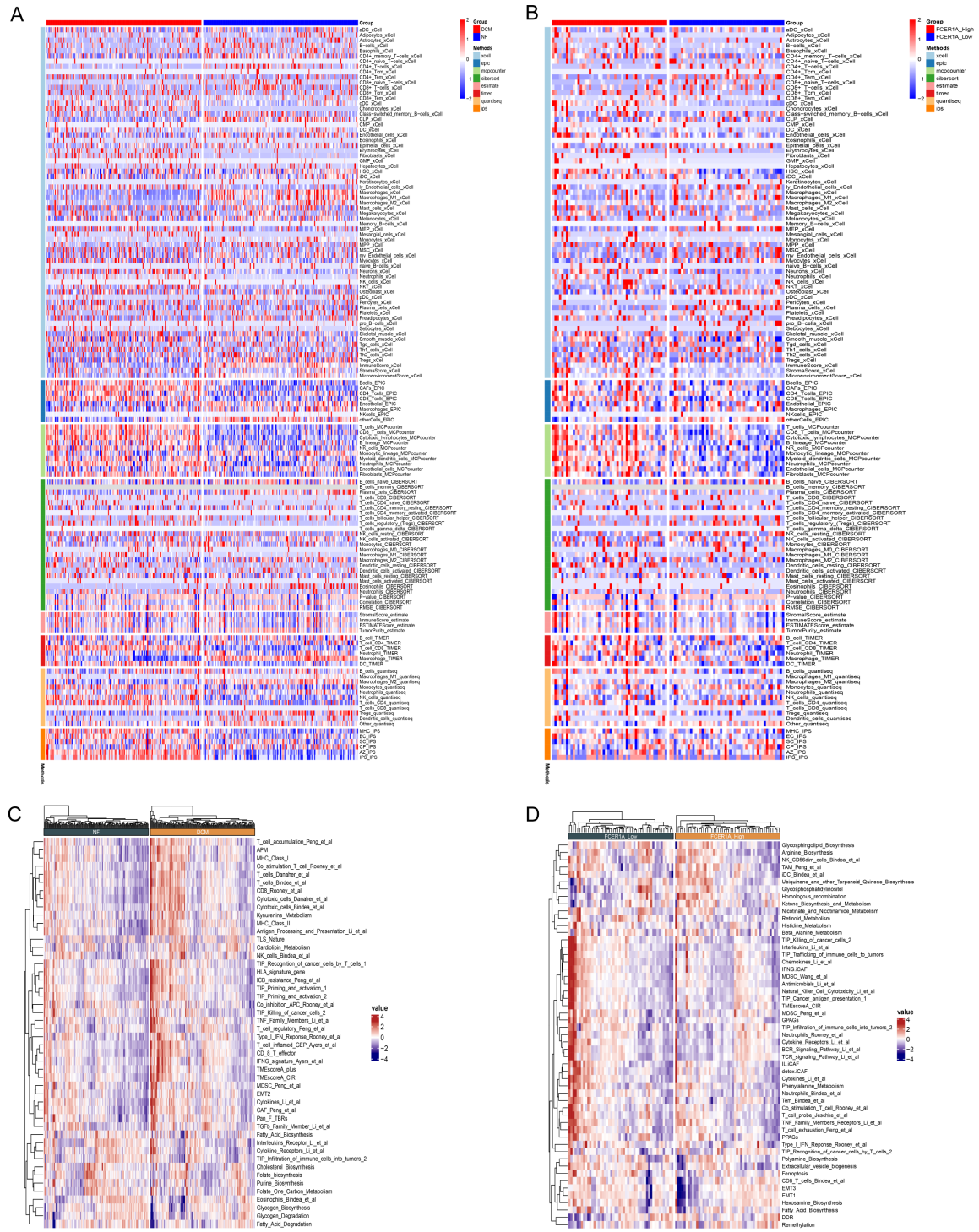

Figure 6. Decoding of the immune microenvironment associated with DCM and FCER1A. A. Heatmap of immune cell infiltration grouped by DCM and NF. B. Heatmap of immune cell infiltration grouped by high and low FCER1A expression. C. Heatmap of immune-related feature expression grouped by DCM and NF. D. Heatmap of immune-related feature expression grouped by high and low FCER1A expression.

genes were used for modelling. Interestingly, on the one hand, the models built with the intersecting genes performed very well in both the training and validation sets, with AUCs

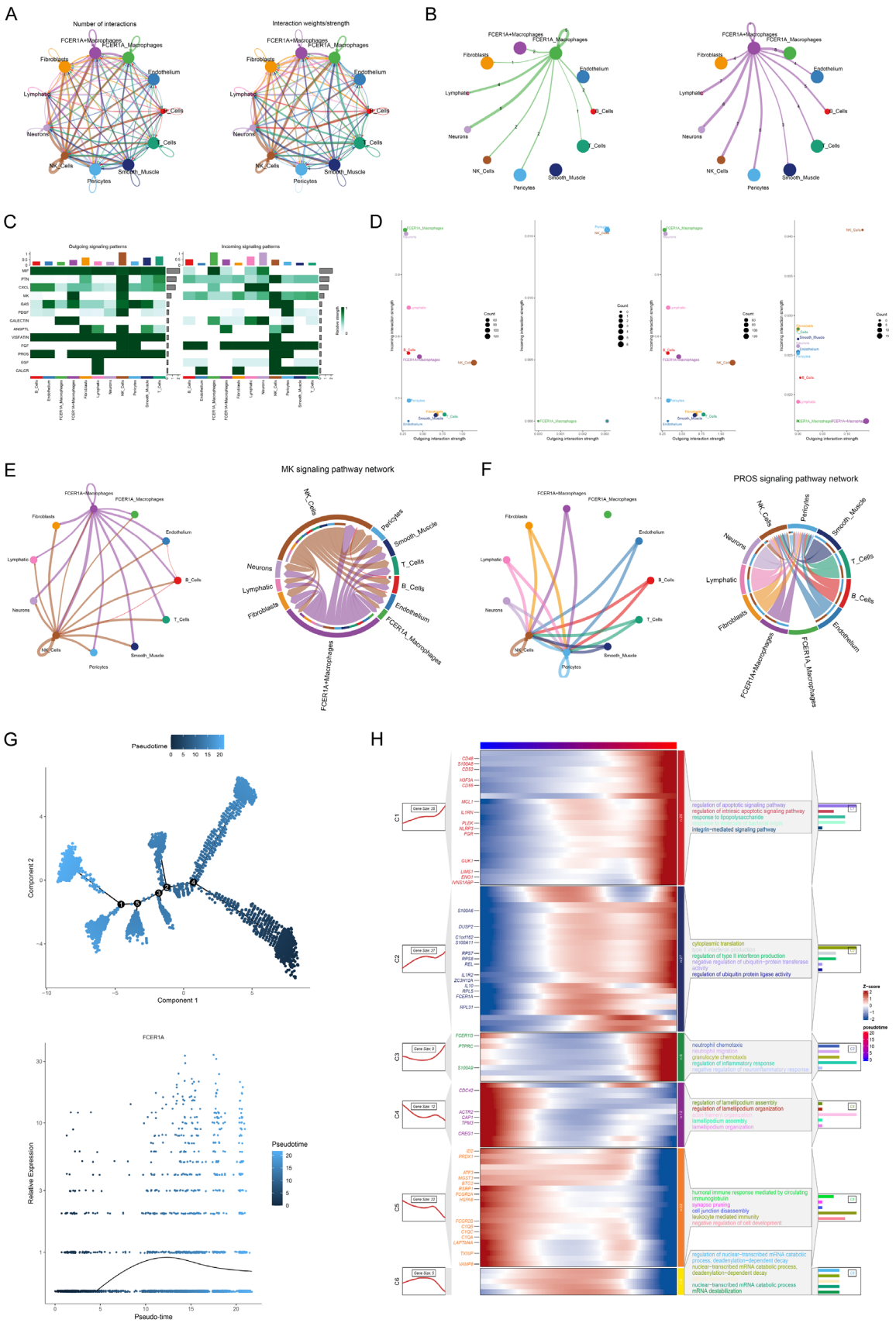
A
Number of interactions
Interaction weights/strength
B
C
Outgoing signaling patterns
Incoming signaling patterns
D
E
MK signaling pathway network
F
PROS signaling pathway network
G
Pseudotime
Component 1
Component 2
FCER1A
Relative Expression
Pseudo-time
H
Z-score
pseudotime

Figure 7. Analysis of the cellular microenvironment of FCER1A+ macrophages in DCM. A. Network graph of interaction strengths between different cell clusters. B. Network plot of interaction strengths between FCER1A+ and FCER1A- macrophages and other cells. C. Heat map of differences in receptor-ligand interactions between different cell clusters. D. Differences in the entry and exit situations of different cell clusters in the MK and PROS pathways. E. Network and chord diagrams of cell entry and exit in the MK pathway. F. Network and chord diagrams of cell entry and exit in the PROS pathway. G. Analysis of the differentiation pathway of macrophages in DCM and the expression pathway of FCER1A. H. Heatmap of differential expression of pseudotime genes during differentiation.

A

gene	drug	regulatory.approval	indication	interaction.score
FCER1A	SLM6071469	Not Approved		1.875274
FCER1A	SLC4101431	Not Approved		1.875274
FCER1A	MP-A08	Not Approved		1.875274
FCER1A	OPAGANIB	Not Approved		1.875274
FCER1A	COMPOUND 59 [PMID: 30889352]	Not Approved		1.875274
FCER1A	BENZYLPENICILLOYL POLYLYSINE	Approved	Diagnostic Agents	3.750548
FCER1A	PF-543	Not Approved		1.875274
FCER1A	OMALIZUMAB	Approved	antiasthmatic agent	0.937637
FCER1A	ROME	Not Approved		3.750548
FCER1A	COMPOUND 49 [PMID: 30889352]	Not Approved		1.875274
FCER1A	COMPOUND 27D [PMID: 28231433]	Not Approved		1.875274
FCER1A	COMPOUND 60 [PMID: 30889352]	Not Approved		1.875274
FCER1A	SKI II	Not Approved		1.250183
FCER1A	COMPOUND 55 [PMID: 30889352]	Not Approved		1.875274

B

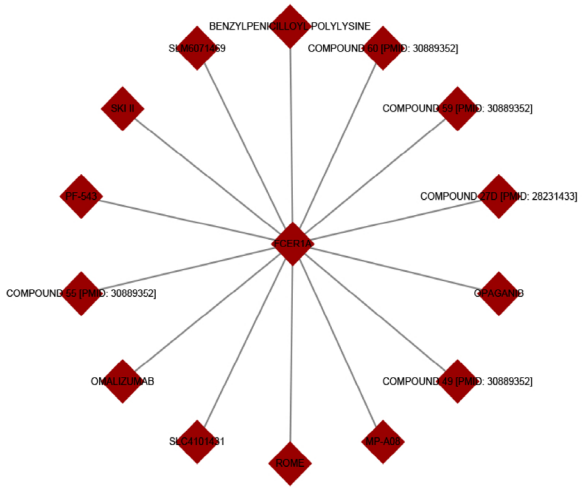

Figure 8. Small molecule drug screening for FCER1A. A. Drugs against FCER1A in the DGIdb database. B. Interaction network graph between FCER1A and drugs.

greater than 0.8 in the training set and calibration curves close to the ideal line in the validation set. On the other hand, FCER1A showed the best performance in multiple models, making it the most critical gene identified in this study for the occurrence of diseases such as SLE and DCM.

The Fc fragment of IgE, high-affinity I, receptor for; alpha polypeptide (FCER1A) gene encodes the alpha subunit of the high-affinity IgE receptor (FcεRI), which plays a critical role in immune responses [27]. This receptor is predominantly expressed on the surface of mast cells and basophils and mediates allergic reactions upon binding to IgE [28]. Recent studies have also implicated FCER1A in the pathogenesis of SLE [29]. In mononuclear phagocytes, such as macrophages and dendritic cells, FCER1A has been shown to influence antigen processing and presentation, as well as cytokine production [30]. In our study, the SMR result further supports the role of FCER1A in lupus by identifying polymorphisms in the FCER1A gene that are associated with the risk of developing SLE.

FCER1A encodes the alpha subunit of the high-affinity IgE receptor (FcεRI), which is primarily expressed on mast cells and basophils [31-33]. It binds IgE antibodies and triggers cell activation upon allergen recognition, leading to the release of inflammatory mediators (e.g. histamine) that drive allergic responses [31-33]. This gene plays a key role in type I hypersensitivity (e.g., asthma, anaphylaxis) and anti-parasitic immunity, making it a potential therapeutic target for allergic diseases. Genetic variations in FCER1A are associated with allergy susceptibility [31-33]. Through our analysis, we found that FCER1A plays a very important role in DCM patients. First, FCER1A is highly expressed in several conventional transcriptome datasets in DCM patients, which is also confirmed at the single-cell level. Second, FCER1A is highly expressed in macrophages and can upregulate several immune-related pathways, such as PI3K, NFKB, Toll-like receptors, and multiple immune cell activation pathways. Third, high expression of FCER1A is closely associated with high infiltration of various immune cells into the ventricle, such as NK cells, T cells, DC cells and macrophages. Fourth, within the ventricular microenvironment, FCER1A+ macrophages have stronger interactions with other cells compared to FCER1A- macrophages, mainly enriched in the MF and PROS pathways. Fifth, the FCER1A gene is mainly expressed in the middle and late stages of mononuclear macrophage differentiation, and its combined expression trend with other genes may enrich pathways such as type II interferon regulation. Sixth, FCER1A mainly serves as a risk factor for the occurrence of SLE, and its increased expression significantly increases the possibility of SLE. Based on the above findings, we have fully demonstrated the key role of the FCER1A gene in the DCM ventricular microenvironment and obtained small molecule drugs targeting FCER1A, such as BENZYLPENICILLOYL POLYLYSINE and OMALIZUMAB, providing important guidance for clinical medication. In conclusion, our study provides new insights into the link between SLE and DCM and shows that FCER1A may be a potential key factor in both diseases, playing an important role in the immune response.

Conclusions

In conclusion, mononuclear macrophages are significantly increased in DCM samples compared to NF samples, and the FCER1A gene is significantly highly expressed in mononuclear macrophages. Its high expression in DCM may upregulate related pathways represented by immune activation and enhance the interaction strength between mononuclear macrophages and other ventricular cells to play an important function. Considering the significant role of FCER1A in DCM, we have obtained its targeted drugs, providing hope for clinical drugs to treat DCM.

Acknowledgements

This study was sponsored by Anyue County People's Hospital.

Disclosure of conflict of interest

None.

Address correspondence to: Tao Wu, Department of Cardiovascular Medicine, People's Hospital of Anyue County, Ziyang 642350, Sichuan, PR China. E-mail: 18349376435@163.com

References

[1] Zhao X, Liu S, Wang X, Chen Y, Pang P, Yang Q, Lin J, Deng S, Wu S, Fan G and Wang B. Dia-

betic cardiomyopathy: clinical phenotype and practice. Front Endocrinol (Lausanne) 2022; 13: 1032268.
[2] Hershberger RE, Hedges DJ and Morales A. Dilated cardiomyopathy: the complexity of a diverse genetic architecture. Nat Rev Cardiol 2013; 10: 531-547.
[3] Peng C, Zhang Y, Lang X and Zhang Y. Role of mitochondrial metabolic disorder and immune infiltration in diabetic cardiomyopathy: new insights from bioinformatics analysis. J Transl Med 2023; 21: 66.
[4] Li S, Liu S, Sun X, Hao L and Gao Q. Identification of endocrine-disrupting chemicals targeting key DCM-associated genes via bioinformatics and machine learning. Ecotoxicol Environ Saf 2024; 274: 116168.
[5] Japp AG, Gulati A, Cook SA, Cowie MR and Prasad SK. The diagnosis and evaluation of dilated cardiomyopathy. J Am Coll Cardiol 2016; 67: 2996-3010.
[6] Jesus D, Matos A, Henriques C, Zen M, Larosa M, Iaccarino L, Da Silva JAP, Doria A and Ines LS. Derivation and validation of the SLE Disease Activity Score (SLE-DAS): a new SLE continuous measure with high sensitivity for changes in disease activity. Ann Rheum Dis 2019; 78: 365-371.
[7] Pan L, Lu MP, Wang JH, Xu M and Yang SR. Immunological pathogenesis and treatment of systemic lupus erythematosus. World J Pediatr 2020; 16: 19-30.
[8] Wang B, Hu S, Shi D, Bing Z and Li Z. Arrhythmia and/or cardiomyopathy related to maternal autoantibodies: descriptive analysis of a series of 16 cases from a single center. Front Pediatr 2019; 7: 465.
[9] Chen DY, Chen YM, Tzang BS, Lan JL and Hsu TC. Th17-related cytokines in systemic lupus erythematosus patients with dilated cardiomyopathies: a possible linkage to parvovirus B19 infection. PLoS One 2014; 9: e113889.
[10] Lai H, Cheng X, Liu Q, Luo W, Liu M, Zhang M, Miao J, Ji Z, Lin GN, Song W, Zhang L, Bo J, Yang G, Wang J and Gao WQ. Single-cell RNA sequencing reveals the epithelial cell heterogeneity and invasive subpopulation in human bladder cancer. Int J Cancer 2021; 149: 2099-2115.
[11] Molina-Navarro MM, Rosello-Lleti E, Ortega A, Tarazon E, Otero M, Martinez-Dolz L, Lago F, Gonzalez-Juanatey JR, Espana F, Garcia-Pavia P, Montero JA, Portoles M and Rivera M. Differential gene expression of cardiac ion channels in human dilated cardiomyopathy. PLoS One 2013; 8: e79792.
[12] Jia C, Guan W, Yang A, Xiao R, Tang WH, Moravec CS, Margulies KB, Cappola TP, Li M and Li C. MetaDiff: differential isoform expression analysis using random-effects meta-regression. BMC Bioinformatics 2015; 16: 208.
[13] Liu Y, Morley M, Brandimarto J, Hannenhalli S, Hu Y, Ashley EA, Tang WH, Moravec CS, Margulies KB, Cappola TP and Li M; MAGNet consortium. RNA-Seq identifies novel myocardial gene expression signatures of heart failure. Genomics 2015; 105: 83-89.
[14] Sweet ME, Cocciolo A, Slavov D, Jones KL, Sweet JR, Graw SL, Reece TB, Ambardekar AV, Bristow MR, Mestroni L and Taylor MRG. Transcriptome analysis of human heart failure reveals dysregulated cell adhesion in dilated cardiomyopathy and activated immune pathways in ischemic heart failure. BMC Genomics 2018; 19: 812.
[15] Tan WLW, Anene-Nzelu CG, Wong E, Lee CJM, Tan HS, Tang SJ, Perrin A, Wu KX, Zheng W, Ashburn RJ, Pan B, Lee MY, Autio MI, Morley MP, Tam WL, Cheung C, Margulies KB, Chen L, Cappola TP, Loh M, Chambers J, Prabhakar S and Foo RSY; Charge-Heart Failure Working Group, CHARGE-EchoGen Consortium. Epigenomes of human hearts reveal new genetic variants relevant for cardiac disease and phenotype. Circ Res 2020; 127: 761-777.
[16] Yamaguchi T, Sumida TS, Nomura S, Satoh M, Higo T, Ito M, Ko T, Fujita K, Sweet ME, Sanbe A, Yoshimi K, Manabe I, Sasaoka T, Taylor MRG, Toko H, Takimoto E, Naito AT and Komuro I. Cardiac dopamine D1 receptor triggers ventricular arrhythmia in chronic heart failure. Nat Commun 2020; 11: 4364.
[17] Flam E, Jang C, Murashige D, Yang Y, Morley MP, Jung S, Kantner DS, Pepper H, Bedi KC Jr, Brandimarto J, Prosser BL, Cappola T, Snyder NW, Rabinowitz JD, Margulies KB and Arany Z. Integrated landscape of cardiac metabolism in end-stage human nonischemic dilated cardiomyopathy. Nat Cardiovasc Res 2022; 1: 817-829.
[18] Tao Y, Zhao R, Yang B, Han J and Li Y. Dissecting the shared genetic landscape of anxiety, depression, and schizophrenia. J Transl Med 2024; 22: 373.
[19] Zhu Z, Zhang F, Hu H, Bakshi A, Robinson MR, Powell JE, Montgomery GW, Goddard ME, Wray NR, Visscher PM and Yang J. Integration of summary data from GWAS and eQTL studies predicts complex trait gene targets. Nat Genet 2016; 48: 481-487.
[20] Yu G, Wang LG, Han Y and He QY. clusterProfiler: an R package for comparing biological themes among gene clusters. OMICS 2012; 16: 284-287.
[21] Ritchie ME, Phipson B, Wu D, Hu Y, Law CW, Shi W and Smyth GK. Limma powers differential expression analyses for RNA-sequencing

and microarray studies. Nucleic Acids Res 2015; 43: e47.
[22] Zeng D, Ye Z, Shen R, Yu G, Wu J, Xiong Y, Zhou R, Qiu W, Huang N, Sun L, Li X, Bin J, Liao Y, Shi M and Liao W. IOBR: multi-omics immuno-oncology biological research to decode tumor microenvironment and signatures. Front Immunol 2021; 12: 687975.
[23] Gu Z, Eils R and Schlesner M. Complex heatmaps reveal patterns and correlations in multidimensional genomic data. Bioinformatics 2016; 32: 2847-2849.
[24] Jin S, Guerrero-Juarez CF, Zhang L, Chang I, Ramos R, Kuan CH, Myung P, Plikus MV and Nie Q. Inference and analysis of cell-cell communication using CellChat. Nat Commun 2021; 12: 1088.
[25] Nukui T and Onogi A. An R package for ensemble learning stacking. Bioinform Adv 2023; 3: vbad139.
[26] Zhu Y, Yang X and Zu Y. Integrated analysis of WGCNA and machine learning identified diagnostic biomarkers in dilated cardiomyopathy with heart failure. Front Cell Dev Biol 2022; 10: 1089915.
[27] Sharma V, Michel S, Gaertner V, Franke A, Vogelberg C, von Berg A, Bufe A, Heinzmann A, Laub O, Rietschel E, Simma B, Frischer T, Genuneit J, Potaczek DP and Kabesch M. A role of FCER1A and FCER2 polymorphisms in IgE regulation. Allergy 2014; 69: 231-236.
[28] Andiappan AK, Puan KJ, Lee B, Yeow PT, Yusof N, Merid SK, Kumar D, Lum J, Foo S, Koh G, Poidinger M, Zolezzi F; eQTLGen Consortium; BIOS Consortium, Wang Y, Melen E and Rotzschke O. Inverse association of FCER1A allergy variant in monocytes and plasmacytoid dendritic cells. J Allergy Clin Immunol 2021; 147: 1510-1513, e8.
[29] Yang J, Lu MM, Lu YW, Feng CC, Leng RX, Pan HF and Ye DQ. Sex-specific differences in the relationship between the single-nucleotide polymorphism rs2298804 of FCER1A and the susceptibility to systemic lupus erythematosus in a Chinese Han population. Clin Exp Dermatol 2013; 38: 410-416.
[30] Guo Q, Fan YN, Xie M, Wang QN, Li J, Liu S, Wang X, Yu D, Zou Z, Gao G, Zhang Q, Hao F, Feng J, Yang R, Wang M, Fu H, Bao X and Duan L. Exploring the transcriptomic landscape of moyamoya disease and systemic lupus erythematosus: insights into crosstalk genes and immune relationships. Front Immunol 2024; 15: 1456392.
[31] Odell ID. Cross-tissue organization of myeloid cells in scleroderma and related fibrotic diseases. Curr Opin Rheumatol 2024; 36: 379-386.
[32] Liang Y, Chang C and Lu Q. The genetics and epigenetics of atopic dermatitis-filaggrin and other polymorphisms. Clin Rev Allergy Immunol 2016; 51: 315-328.
[33] Eming R and Hertl M. Immunoadsorption in pemphigus. Autoimmunity 2006; 39: 609-16.